J-1-2

URCAT (U-shaped-Recess-Channel-Array Transistor) Technology for 60nm DRAM and beyond

Chihoon Lee, J.C. Park, S. H. Park*, S. S. Lee, S. D. Hong**, I. G. Kim, Y. J. Choi, T. W. Lee, G. Y. Jin, and Kinam Kim

DRAM PM Center, DRAM PA Team*, CAE**, Samsung Electronics Co., San#16, Banwol-Ri, Taean-Eup, Hwaseong-City, Geonggi-Do, 445-701, KOREA, e-mail: chihoon.lee@samsung.com

Abstract

For the first time, U-RCAT (U-shaped-Recess-Channel-Array Transistor) technology has been developed in a 1Gb density DRAM with 60nm feature size and beyond. The U-RCAT shows superior characteristics such as sub-threshold swing (*SW*), gate induced drain leakage (*GIDL*), operating current, *DIBL*, junction leakage current, data retention time, and Fowler-Nordheim (*FN*) stress immunities compared with the S-RCAT (Sphere-shaped--Recess-Channel-Array Transistor) structure due to the relaxed *E-field* intensity from the smooth and enlarged neck curvature. In this paper, the U-RCAT is argued to be the most promising DRAM array transistor suitable for highly reliable cell array transistors with sub-60 nm features and beyond.

Introduction

As the minimum feature size of DRAM shrinks from 110nm to the sub-50nm era, it is more difficult to get suitable data retention time and performance out of cell array transistors. RCAT (Recess-Channel-Array Transistor) [1] have been applied to increase the effective channel length (L_{eff}) by 80nm. Also, S-RCAT has been used to increase the data retention time using the spherical ball part for a 70nm channel length increase [Table 1]. In the S-RCAT structure, however, the neck curvature is inevitable due to the dual structure forming the upper neck part and the lower ball part (playing the role of channel) [Fig. 1 (a)]. Although S-RCAT shows good performance with low operating voltage [2], it has frail long-term reliability due to the highly concentrated electrical field (*E-field*) at the stiff neck curvature [Fig. 1 (b)]. It has been shown that the immense *E-field* intensity is concentrated at the stiff curvature region rather than the ball side and bottom in the S-RCAT through device simulation [Fig. 1 (c)]. In addition, there are concerns about the S-RCAT's scale-down ability under 50nm feature size era.

In this paper, a novel and manufacturable U-RCAT is proposed as the cell array structure with drastically enhanced long-term reliability by relaxing the *E-field* at the neck curvature, estimating FN-stress immunities. The data retention time of the optimal U-RCAT design will also be discussed.

Experimental and Results

1. Fabrication Processes

The novel and manufacturable U-RCAT is integrated on a p-type bulk Si (100) wafer and the process flow is illustrated in Fig. 2. The hard mask to pattern the U-RCAT structure is deposited and etched using conventional photolithography after defining the active region [Fig. 2 (a)]. The upper neck part is formed by a Si recess etching [Fig. 2 (b)]. It is trench-etched by using an anisotropic etching process. The thin thermal oxide is deposited to protect the neck part during ball etching [Fig. 2 (c)]. The neck spacer is made by thin oxide etching [Fig. 2 (d)]. The ball part of U-RCAT is formed by using two etching steps compared to the S-RCAT which only uses an isotropic etching. In the U-RCAT process, two step etching is the core process. First, anisotropic etching is progressed and in-situ followed by isotropic etching to make the ball part [Fig. 2 (e) ~ (f)]. On the other hand, in the S-RCAT process, the neck part has the bowing profile due to the scattering of the etching gas resulting from the narrow open area and deep depth in the design rule of sub-60nm. The bowing in the neck part directly gives rise to the higher *E-field* by narrowing the angle of the neck curvature. The depth of the neck part in the U-RCAT is reduced by approximately 50% compared to S-RCAT. This will increase the angle of the neck curvature which will cause the decreased *E-field* shown below in the electricity and reliability results. U-RCAT is realized by wet etching the remaining spacer thin oxide [Fig. 2 (g)]. The gate stack is formed by using conventional polycide ($Si(100)/G_{ox}/n^+$ doped poly/WSi_x/SiN_x) [Fig. 2 (h)]. Fig.3 is the vertical SEM image of the U-RCAT after forming the gate stack. Fig. 4 shows high resolution TEM images of S-RCAT and U-RCAT after gate poly deposition. The neck curvature of U-RCAT is 120~130° compared with 100~110° in the S-RCAT and enlarged by approximately 20% without the thickness.

2. Electrical Characteristics

The V_{th} distributions and the correlation of the operating current (I_{on}) vs. V_{th} are shown in Fig. 5-6. At first, the V_{th} of the U-RCAT decreases by 60mV/cell (6.7%) and I_{on} gains 0.5uA/cell (7.6%) with the same cell channel doping condition, which is caused by the enlarged channel width and flatter bottom channel region. U-RCAT has the lower V_{th} due to the improved *SW* and *DIBL*, which means it can be operated at a lower voltage compared to S-RCAT. *SW* and *DIBL* are improved by 3.5 % from 112mV/dec to 108mV/dec and by 9% from 32.5mV to 29.5mV, respectively, due to the flatter ball bottom channel with higher drivability [3] and longer L_{eff} [Fig.7-8]. *Body effect* decreased from 0.45V/Vb to 0.39V/Vb, which increases the data retention time due to the lower word-line boosting voltage [Fig. 9]. *GIDL* is also improved by 15% from 0.13 pA/cell to 0.11 pA/cell, which allows for longer data retention time [Fig. 10]. Cell array junction leakage of the U-RCAT decreases by 25% from 2.7×10^{-16}A/cell to 2.0×10^{-16}A/cell due to the neck curvature part from the junction region and the narrower junction area compared to that of the S-RCAT [Fig. 11].

3. Data retention time

There are some important factors that make an effect on the data retention time such as *SW*, *GIDL*, *DIBL*, *body effect*, and junction leakage current. Although U-RCAT and S-RCAT are treated by the same channel doping conditions, the data retention time of the U-RCAT is relatively improved by over 20% before *FN* stress (*tRC* 10min), and by 50% after *FN* stress compared to that of the S-RCAT [Fig. 12]. This means that the data retention time must be influenced by the above improved electrical characteristics resulting from the *E-field* relaxation at the neck curvature near junction region.

4. FN stress immunities and U-RCAT design

In order to estimate the long-term reliability of the U-RCAT, FN stress immunities are measured at 85°C from 5V to 6V for 60 seconds and the correlation between *SW* vs. V_{th} and the charge pumping current (*ICP*) distributions with FN stress are measured [Fig. 13-14]. Their variations are relatively very low and stable in the U-RCAT as FN stress voltages increases. This indicates that the U-RCAT structure must be an improvement for long-term reliability. Ball depth and diameter are simulated to design the optimal U-RCAT profile for the best reliable performance [Fig. 15]. The *E-field* intensity hardly varies in the neck curvature variations (120-130°) under the manufacturable U-RCAT range. But, the data retention time is sensitively degraded under 120° as the ball diameter decreased and the ball depth increased due to the degradation of the *SW*, *DIBL*, and junction leakage current. The well-designed U-RCAT shows much less *E-field* at the neck curvature [Fig. 15 (d-e)].

Conclusion

The U-RCAT structure is shown to have been successfully developed to enhance the frail long-term reliability of the S-RCAT. U-RCAT is a drastic improvement over S-RCAT due to the *E-field* relaxation by enlarging the angle of the stiff neck curvature. U-RCAT shows the superior electrical characteristics such as I_{on} current gain, *SW*, *DIBL*, *GIDL*, *body effect*, and junction leakage current due to the increased channel width, the reduced junction area, and the relaxed *E-field intensity*. The data retention time is also improved due to the lower *SW* and junction leakage current.

Reference

[1] J.Y.Kim et al., Symp. On VLSI Tech., pp.11-12, 2003
[2] J.Y.Kim et al., Symp. On VLSI Tech., pp.34-35, 2005
[3] I.G.Kim et al., IEDM., pp.329-332, Dec.2005

Items	110nm		90nm	80nm	70nm	sub_60nm	
Array Transistor	Planar	RCAT	RCAT	RCAT	RCAT	S-RCAT	U-RCAT
Recess Depth	-	150nm	170nm	190nm	200nm	200nm	200nm
Vth	1.3V	1.1V	1.1V	1.2V	1.2V	0.85V	0.80V

Table 1. Transistor types of DRAM cell array with design rule. U-RCAT may be a prominent candidate below 60 nm feature size and beyond. [1]

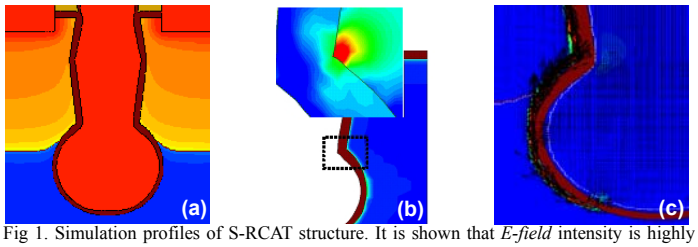

Fig 1. Simulation profiles of S-RCAT structure. It is shown that *E-field* intensity is highly concentrated in the neck curvature due to the stiff neck angle of 100~110˚.

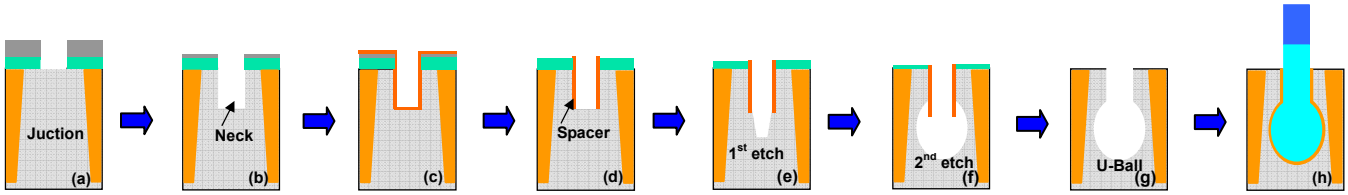

Fig.2 Core process flow of U-RCAT structure. The two step etching processes with different etching rates plays an important role in the formation of the U-RCAT structure. The U-RCAT realizes better performance and reliability with the same area as the S-RCAT, which illustrates the powerful scale-down ability of the U-RCAT versus S-RCAT.

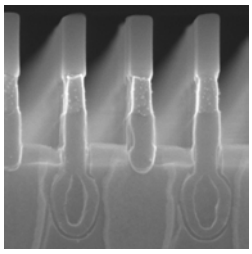

Fig. 3 Vertical SEM image of U-RCAT after forming gate.

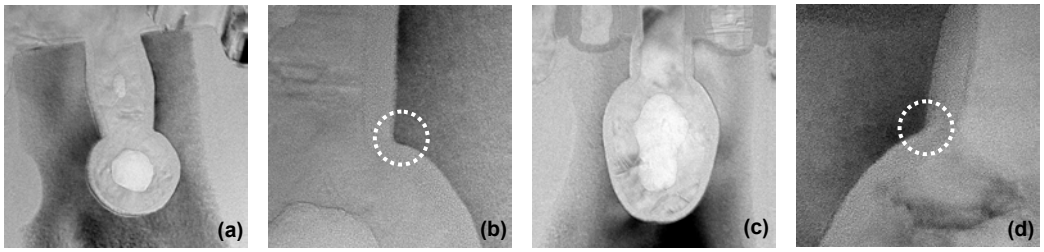

Fig. 4 TEM images of (a) S-RCAT, (b) neck of S-RCAT, (c) U-RCAT, and (d) neck of U-RCAT. The neck curvature of U-RCAT increases by 120~130˚ compared with 100~110˚ in the S-RCAT. U-RCAT shows the smoother and wider neck curvature.

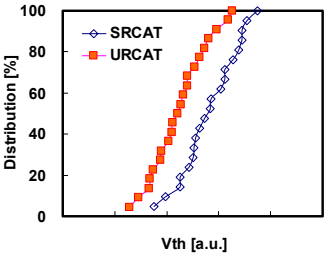

Fig. 5 The V_{th} of the U-RCAT decreased due to the improved SW.

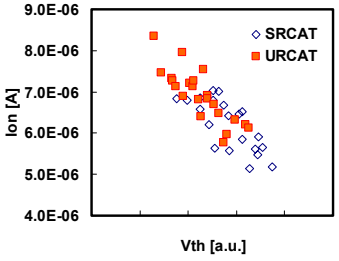

Fig. 6 Correlation curves between the I_{on} *and* V_{th}. The Ion of U-RCAT are enhanced by improving *SW* and *DIBL*.

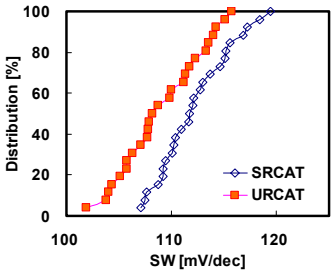

Fig. 7 *SW* Distribution of U-RCAT is improved due to the flatter ball bottom channel and *E-field* relaxation.

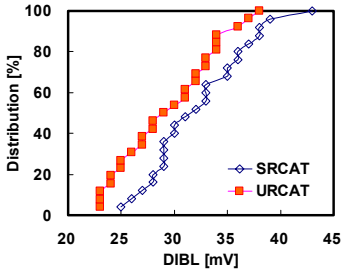

Fig. 8 *DIBL* distribution of the U-RCAT shows better properties than that of S-RCAT due to the increased L_{eff}.

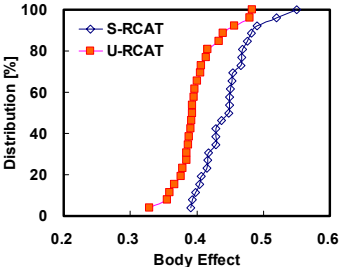

Fig. 9 *Body effect* [$\Delta V_{th}/\Delta V_b$] is improved in the U-RCAT due to greater width.

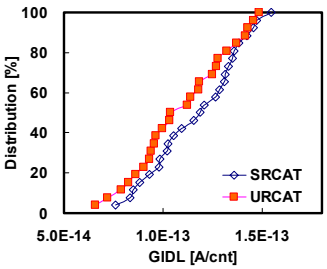

Fig. 10 *GIDL* currents of the U-RCAT are reduced, which helps increase data retention time.

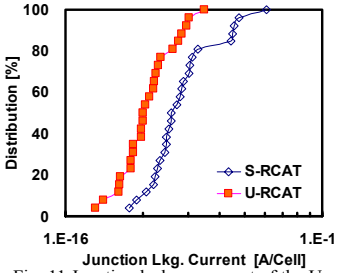

Fig. 11 Junction leakage current of the U-RCAT is improved due to less junction area.

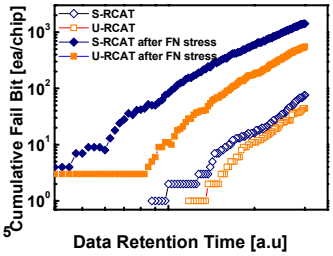

Fig. 12 U-RCAT shows the enhanced data retention time due to the improved *GIDL*, junction leakage current, and the *E-field* relaxation. (*tRC*=10min)

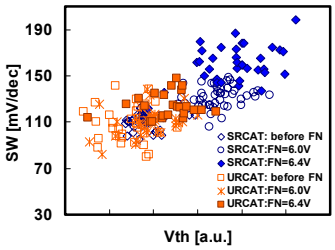

Fig. 13 U-RCAT shows the enhanced *FN* stress immunities due to the relaxed *E-field* at the neck curvature and a better *SW*.

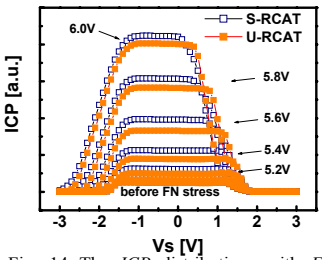

Fig. 14 The *ICP* distributions with *FN stress* are improved in U-RCAT due to less leakage current and smooth neck curvature. (*FN* stress for 60s)

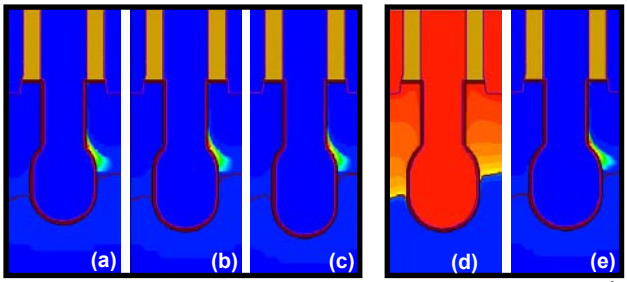

Fig. 15 Device simulation profiles of U-RCAT with ball depth of (a)-100Å, (b)target, (c) +100Å, (d)–(e) the optimal U-RCAT, which shows the least *E-field*. The *E-field* is negligible with the U-ball depth, but the data retention time is very sensitive with the U-ball depth and diameter.